Novel anodic electrochromic aromatic polyamides with multi-stage oxidative coloring based on *N*,*N*,*N*′,*N*′-tetraphenyl-*p*-phenylenediamine derivatives†

Cha-Wen Chang[a] **and Guey-Sheng Liou***[b]

Received 24th June 2008, Accepted 10th September 2008
First published as an Advance Article on the web 22nd October 2008
DOI: 10.1039/b810750e

A series of novel aromatic polyamides with pendent 4,4′-dimethoxy-substituted triphenylamine (TPA) units were prepared *via* the direct phosphorylation polycondensation from a new dicarboxylic acid monomer, *N*,*N*-bis(4-carboxyphenyl)-*N*′,*N*′-di(4-methoxyphenyl)-1,4-phenylenediamine (**4**), and various aromatic diamines. These polyamides were amorphous with good solubility in many organic solvents, such as *N*-methyl-2-pyrrolidinone (NMP) and *N*,*N*-dimethylacetamide (DMAc), and could be solution-cast into flexible polymer films. They had excellent levels of thermal stability associated with their relatively high glass-transition temperatures (233–308 °C). These polymers exhibited strong UV-vis absorption bands at 351–363 nm in NMP solution. Their photoluminescence spectra showed maximum bands around 450–504 nm. The hole-transporting and electrochromic properties are examined by electrochemical and spectroelectrochemical methods. Cyclic voltammograms of the polyamide **6g** prepared from the dicarboxylic acid monomer (**4**) with a structurally similar diamine monomer *N*,*N*-bis(4-aminophenyl)-*N*′,*N*′-di(4-methoxyphenyl)-1,4-phenylenediamine (**5g**) exhibited four reversible oxidation redox couples in acetonitrile solution at $E_{onset} = 0.35$, $E_{1/2} = 0.64$, 0.84, and 0.99 V, respectively. After over 3000 cyclic switches for green color, the films of polyamide **6g** still showed excellent continuous cyclic stability of electrochromism.

Introduction

Electrochromism involves electroactive materials that present a reversible change in optical properties when the material is electrochemically oxidized or reduced. A single-species electrochromic material which exhibits several colors could be termed as "polyelectrochromic".[1] Electrochromic properties have proved especially useful or promising for the construction of mirrors,[2] displays,[3–5] windows,[6–10] and earth-tone chameleon materials.[11–13] On the basis of this concept, electrochromic rear-view and side-view mirrors have been recently commercialized in the automotive industry.[14,15] Anodic electrochromic materials are those that exhibit different colors depending upon their oxidation states. One of the interesting multicolor systems is that based upon the *N*,*N*,*N*′,*N*′-tetraphenyl-*p*-phenylenediamine moiety.[16] Therefore the intramolecular electron transfer and electronic coupling effects in the oxidized states are important in the design of new *N*,*N*,*N*′,*N*′-tetraphenyl-*p*-phenylenediamine based polymers for electrochromic devices.

Intramolecular electron transfer (ET) processes have been studied extensively in mixed-valence (MV) systems.[17–19] They usually employ one-dimensional MV compounds containing two or more redox states connected *via* a σ- or π-bridge molecule. According to Robin and Day,[20] MV systems can be classified into three categories: class I with practically no coupling between the different redox states, class II with moderate electronic coupling, and class III with strong electronic coupling (the electron is delocalized over the two redox centers). Recently, an experimental and theoretical study of the *N*,*N*,*N*′,*N*′-tetraphenyl-*p*-phenylenediamine cation radical has been reported and a symmetrical delocalized class III structure was proposed.[21] The redox properties, ion-transfer process, electrochromism, and photoelectrochemical behavior of *N*,*N*,*N*′,*N*′-tetrasubstituted-1,4-phenylenediamine are important for technological applications.[22–26]

In order to be useful for applications, electrochromic materials must exhibit long-term stability, multiple colors with the same material, and large changes in transmittance (large Δ%T) between their bleached and colored states.[27] Our strategy was to synthesize *N*,*N*,*N*′,*N*′-tetrasubstituted-1,4-phenylenediamine monomers such as diamines and dicarboxylic acids into which phenyl groups were incorporated by electron-donating substituents at the *para*-position of TPA; coupling reactions were largely prevented by affording stable cationic radicals and lowering the oxidation potentials.[28–31] The corresponding polymers with high molecular weights and high thermal stability could be obtained through conventional polycondensation techniques. Because of the incorporation of packing-disruptive, propeller-shaped TPA units along the polymer backbone, most of these polymers exhibited good solubility in polar organic solvents and uniform, transparent amorphous thin films could be obtained by solution casting and spin-coating methods. This is advantageous for their ready fabrication of large-area, thin-film devices.

[a]*Department of Applied Chemistry, National Chi Nan University, 1 University Road, Puli, Nantou Hsien, 54561, Taiwan, Republic of China*
[b]*Institute of Polymer Science and Engineering, National Taiwan University, Taipei, 10617, Taiwan, Republic of China. E-mail: gsliou@ntu.edu.tw*

† Electronic supplementary information (ESI) available: Further synthesis details; NMR, COSY, HMQC spectra; DSC curves; IR spectra; tables of solubility, viscosity and GPC data; WAXD pattern; TMA and TGA plots; UV-vis spectra; CVs. See DOI: 10.1039/b810750e

In this article, we therefore synthesized a new diacid, *N*,*N*-bis(4-carboxyphenyl)-*N*′,*N*′-di(4-methoxyphenyl)-1,4-phenylenediamine (**4**), and its derived polyamides containing one or two *N*,*N*,*N*′,*N*′-tetraphenyl-*p*-phenylenediamine units that have multiple redox potentials to produce multiple colors. The general properties such as solubility and thermal properties are described. The electrochemical and electrochromic properties of these polymers are also investigated herein and are compared with those of structurally related ones from model compounds **M1**, **M2** and polyamides **M3** and **M4**.[32]

Experimental

Materials

According to well-known chemistry,[33–35] 4-aminotriphenylamine (mp = 148–149 °C) was prepared by the aromatic nucleophilic amination of 4-nitrofluorobenzene and diphenylamine in *N*,*N*-dimethylformamide (DMF) in the presence of sodium hydride, followed by reduction by means of hydrazine and Pd/C in refluxing ethanol. 4-Amino-4′,4″-dimethoxytriphenylamine (**2**) was prepared by the potassium carbonate-mediated aromatic nucleophilic substitution reaction of 4-nitroaniline with iodoanisole[36] followed by hydrazine Pd/C-catalytic reduction according to the synthesis route outlined in Scheme 1. 4,4′-Diaminotriphenylamine[32b] (**5d**; mp = 186–187 °C), 4,4′-diamino-4″-methoxytriphenylamine[31] (**5e**; mp = 150–152 °C), *N*,*N*-bis(4-aminophenyl)-*N*′,*N*′-diphenyl-1,4-phenylenediamine[37] (**5f**; mp = 245–247 °C), and *N*,*N*-bis(4-aminophenyl)-*N*′,*N*′-di(4-methoxyphenyl)-1,4-phenylenediamine (**5g**; mp = 87–89 °C)[38] were synthesized by the nucleophilic fluoro-displacement reaction of 4-fluoronitrobenzene with aniline, *p*-anisidine, 4-aminotriphenylamine, and 4-amino-4′,4″-dimethoxytriphenylamine, respectively, followed by palladium-catalyzed hydrazine reduction. Commercially available aromatic diamines such as *p*-phenylenediamine (**5a**), 4,4′-oxydianiline (**5b**), and 9,9-bis(4-aminophenyl)fluorene (**5c**) were purchased from TCI and used as received. Commercially obtained anhydrous calcium chloride ($CaCl_2$) was dried under vacuum at 180 °C for 8 h. Tetrabutylammonium perchlorate (TBAP) (ACROS) was recrystallized twice from ethyl acetate under nitrogen atmosphere and then dried *in vacuo* before use. All other reagents were used as received from commercial sources.

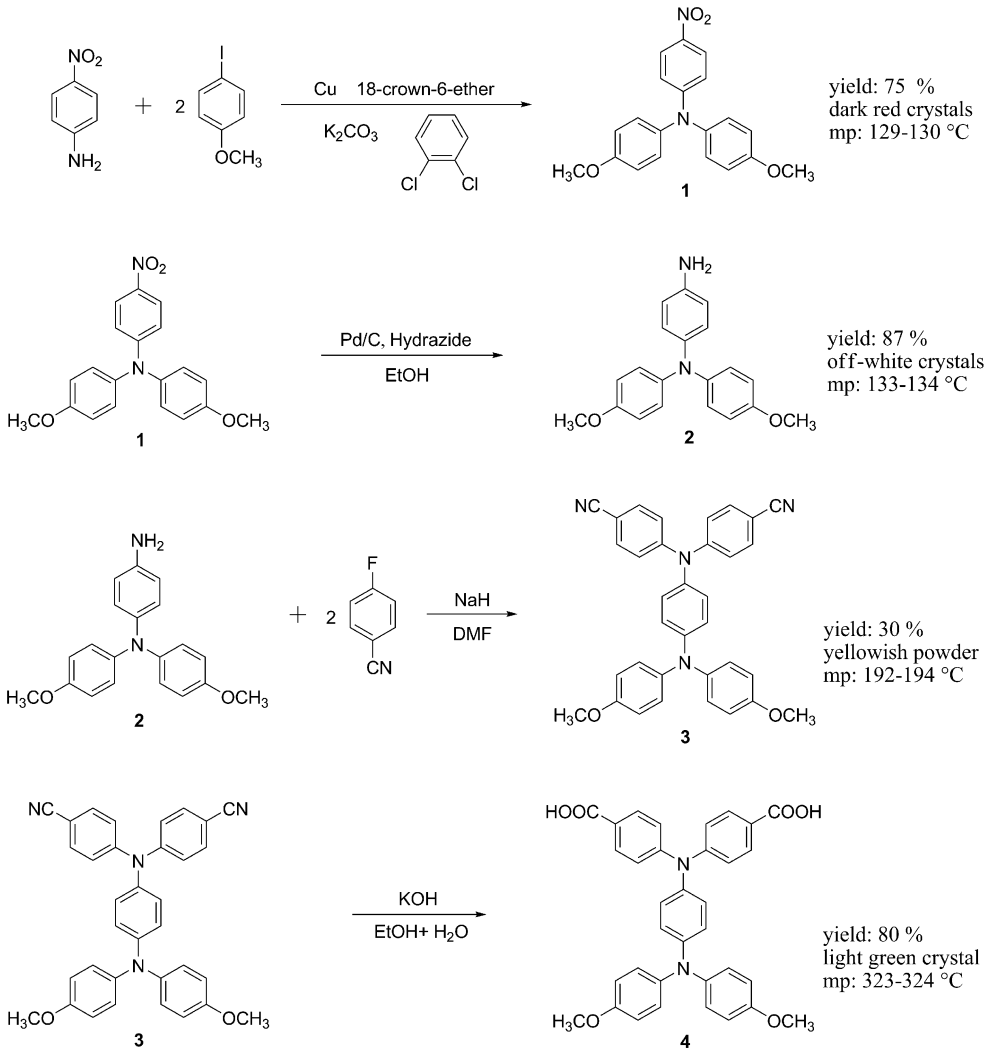

Scheme 1 Synthesis of monomers.

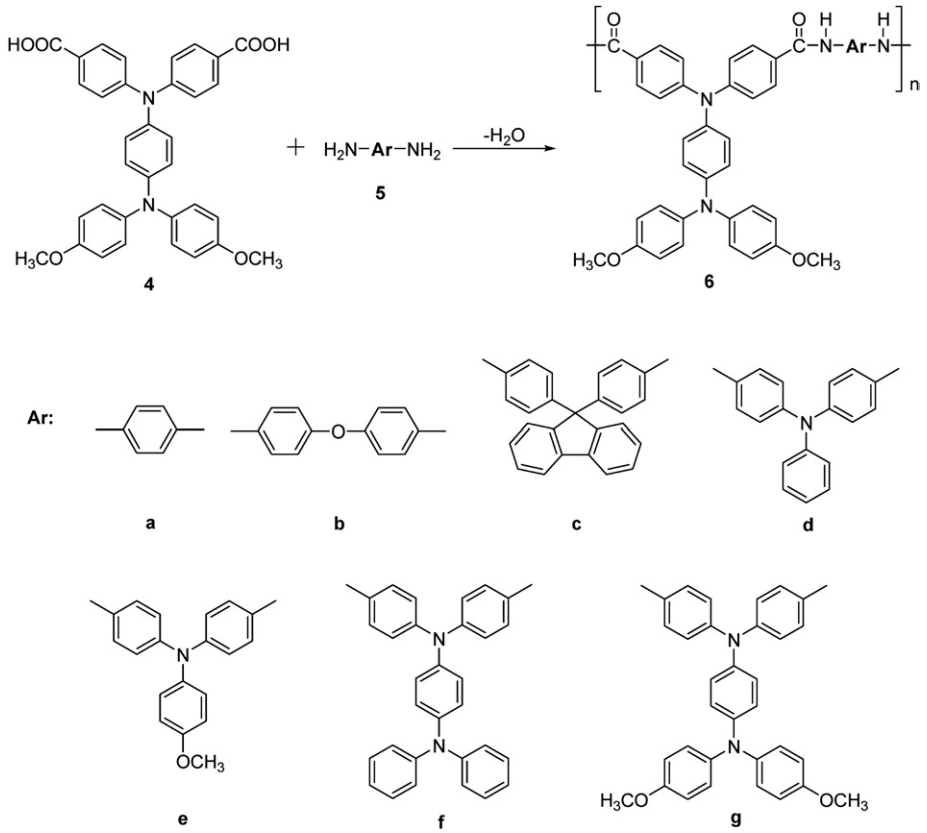

Scheme 2 Synthesis of polyamides by direct polycondensation reaction.

Preparation of the films

A solution of polymer was made by dissolving about 0.60 g of the polyamide sample in 10 mL of *N*,*N*-dimethylacetamide (DMAc). The homogeneous solution was poured into a 9 cm glass Petri dish, which was placed in a 90 °C oven for 5h to remove most of the solvent, then the semi-dried film was further dried *in vacuo* at 170 °C for 7 h. The obtained films were about 50–70μm thick and were used for solubility tests and thermal analyses.

Measurements

Infrared spectra were recorded on a PerkinElmer RXI FT-IR spectrometer. Elemental analyses were run in an Elementar Vario EL-III. ^{1}H and ^{13}C NMR spectra were measured on a Bruker AV-300 and 400 FT-NMR system, and referenced to the $CDCl_3$-d_1 and DMSO-d_6 signals, and peak multiplicity was reported as follows: s, singlet; d, doublet. The inherent viscosities were determined at 0.5 g/dL concentration using a Tamson TV-2000 viscometer at 30 °C. Gel permeation chromatographic (GPC) analysis was performed on a Lab Alliance RI2000 instrument (one column, MIXED-D from Polymer Laboratories) connected with one refractive index detector from Schambeck SFD Gmbh. All GPC analyses were performed using a polymer/DMF solution at a flow rate of 1 mL/min at 70 °C and calibrated with polystyrene standards. Wide-angle X-ray diffraction (WAXD) measurements were performed at room temperature (*ca.* 25 °C) on a Shimadzu XRD-7000 X-ray diffractometer (40 kV, 20 mA), using graphite-monochromatized Cu-Kα radiation. Ultraviolet-visible (UV-vis) spectra of the polymers were recorded on a Varian Cary 50 Probe spectrometer. Thermogravimetric analysis (TGA) was conducted with a Perkin-Elmer Pyris 1 TGA. Experiments were carried out on approximately 4–6 mg film samples heated in flowing nitrogen or air (flow rate = 30 cm^3/min) at a heating rate of 20 °C/min. Thermomechanical analysis (TMA) was conducted with a Perkin-Elmer TMA 7 instrument. The TMA experiments were conducted from 50 to 350 °C at a scan rate of 10 °C/min with

Table 1 Thermal properties of polyamides

Polymer	T_g/°C[a]	T_s/°C[b]	T_d at 5% weight loss/°C[c]		T_d at 10% weight loss/°C[c]		Char yield (wt%)[d]
			N_2	Air	N_2	Air	N_2
6a	266	260	465	480	490	510	68
6b	269	259	485	480	515	530	66
6c	308	294	485	480	525	535	66
6d	262	257	480	480	515	540	71
6e	255	254	485	480	520	520	71
6f	256	243	490	480	525	520	75
6g	233	229	490	475	530	520	73

[a] Midpoint temperature of the baseline shift on the second DSC heating trace (rate = 20 °C/min) of the sample after quenching from 400 to 50 °C (rate = 200 °C/min) in nitrogen. [b] Softening temperature measured by TMA with a constant applied load of 50 mN at a heating rate of 10 °C/min. [c] Decomposition temperature, recorded *via* TGA at a heating rate of 20 °C/min and a gas-flow rate of 30 cm^3/min. [d] Residual weight percentage at 800 °C in nitrogen.

a penetration probe 1.0 mm in diameter under an applied constant load of 50 mN. Softening temperatures (T_ss) were taken as the onset temperatures of probe displacement on the TMA traces. Cyclic voltammetry was performed with a Bioanalytical System Model CV-27 potentiostat and a BAS X–Y recorder with ITO (polymer films area about 0.7 cm × 0.7 cm) was used as a working electrode and a platinum wire as an auxiliary electrode at a scan rate of 50 mV/s against a Ag/AgCl reference electrode in a solution of 0.1 M tetrabutylammonium perchlorate (TBAP)/acetonitrile (CH_3CN). Voltammograms are presented with the positive potential pointing to the left and with increasing anodic currents pointing downward. The spectroelectrochemical cell was composed of a 1 cm cuvette, ITO as a working electrode, a platinum wire as an auxiliary electrode, and an Ag/AgCl reference electrode. Absorption spectra in spectroelectrochemical analysis were measured with a HP 8453 UV-visible spectrophotometer. Photoluminescence spectra were measured with a Jasco FP-6300 spectrofluorometer. Fluorescence quantum yields (Φ_F) values of the samples in NMP were measured by using quinine sulfate in 1 N H_2SO_4 as a reference standard (Φ_F = 0.546).[39,40] All corrected fluorescence excitation spectra were found to be equivalent to their corresponding absorption spectra.

Table 2 Optical properties of polyamides

	Solution λ/nm[a]			Film λ/nm			
Polymer	Abs λ_{max}	PL[b] λ_{max}	Φ_F (%)[c]	λ_0[d]	Abs λ_{max}	Abs λ_{onset}	PL[b] λ_{max}
6a	362	504	1.36	415	354	431	512
6b	351	499	1.43	409	348	426	513
6c	357	499	2.22	405	348	430	511
6d	355	498	1.16	419	350	432	511
6e	360	492	1.18	417	357	436	508
6f	363	483	0.95	419	354	434	514
6g	356	450	0.74	419	359	447	516

[a] Polymer concentration of 10^{-5} mol/L in NMP. [b] They were excited at the abs_{max} for both the solid and solution states. [c] The quantum yield in dilute solution was calculated in an integrating sphere with quinine sulfate as the standard (Φ_F = 0.546). [d] The cutoff wavelength (λ_0) from the UV-vis transmission spectra of polymer films (thickness: 1–3 μm).

Results and discussion

Polymer synthesis

A series of novel aromatic polyamides **6a–6g** having the TPA unit in the main chain and pendent 4,4′-dimethoxy-substituted TPA groups were prepared from the newly synthesized dicarboxylic acid (**4**) (Scheme 1) and various aromatic diamines **5a–5g** by the phosphorylation polycondensation reaction using triphenyl phosphite and pyridine as condensing agents (Scheme 2).[41,42] All the polymerizations proceeded homogeneously throughout the reaction and afforded clear, highly viscous polymer solutions. All the polymers precipitated in a tough, fiber-like form when the resulting polymer solutions were slowly poured with stirring into methanol. These polyamides were obtained in almost quantitative yields, with inherent viscosity values in the range of 0.24–0.83 dL/g. The formation of polyamides was also confirmed by IR and NMR spectroscopy. Fig. S5 (ESI†) shows a typical IR spectrum of polyamide **6b**. The characteristic IR absorption bands of the amide group were around 3414 (N–H stretching) and 1654 cm^{-1} (amide carbonyl). Fig. S6† shows a typical set of ^1H and ^{13}C NMR spectra of polyamide **6b** in DMSO-d_6; all the peaks could be readily assigned to the hydrogen and carbon atoms of the recurring unit. Assignments of each carbon and proton are also assisted by the two-dimensional NMR spectra shown in Fig. S7† and the spectra agree well with the proposed molecular structure of polyamide **6b**. The resonance peaks appearing at 10.13 ppm in the ^1H NMR spectrum and at 164.9 ppm in the ^{13}C NMR spectrum also support the formation of amide linkages.

Table 3 Electrochemical properties of polyamides and model compounds

	Oxidation potential/V (*vs.* Ag/AgCl in CH_3CN)							
	1st		2nd	3rd	4th			
Polymer	$E_{1/2}$	E_{onset}	$E_{1/2}$	$E_{1/2}$	$E_{1/2}$	E_{gap}[a]/eV	HOMO[b] E_{onset}/eV	LUMO[c] E_{onset}/eV
6a	0.61	0.52	0.99	—	—	2.88	4.88	2.00
6b	0.61	0.54	0.98	—	—	2.91	4.90	1.99
6c	0.60	0.52	0.98	—	—	2.88	4.88	2.00
6f	0.62	0.49	—	—	0.98	2.86	4.85	1.99
6g	—	0.35	0.64	0.84	0.99	2.77	4.71	1.94
6′b[d]	0.48	0.36	0.84	—	—	2.95	4.72	1.77

	Oxidation potential/V (*vs.* Ag/AgCl in CH_3CN)	
Polymer	$E_{1/2}$	E_{onset}
M1	0.78	0.70
M2	0.82	0.73
M3	0.82	0.68
M4	1.07	0.90

[a] The data were calculated from polymer film by the equation: gap = $1240/\lambda_{onset}$. [b] The HOMO energy levels were calculated from cyclic voltammetry and were referenced to ferrocene (4.8 eV). [c] LUMO = HOMO − E_{gap}. [d] The value is that of analogous polyamide (**6′b**) with the corresponding -Ar- unit as in the **6** series.

Basic characterization

The solubility behavior of polyamides was tested qualitatively, and the results are summarized in Table S1.† All the polyamides were highly soluble in polar solvents such as NMP, DMAc, DMF, and dimethyl sulfoxide (DMSO), and the enhanced solubility could be attributed to the introduction of the bulky pendent 4,4′-dimethoxy-substituted TPA moiety into the repeat unit. Thus, the excellent solubility makes these polymers potential candidates for practical applications by spin- or dip-coating processes. These polymers could afford transparent, flexible and tough films. In addition, **6c** exhibited better solubility compared to polyamides **6a** and **6b**. This result implies that bulky lateral fluorene groups can provide enhanced solubility because of decreased packing density and crystallinity. The wide-angle X-ray diffraction studies of the polyamides in Fig. S8† indicated that these polymers were essentially amorphous.

The obtained polyamides had inherent viscosities in the range of 0.24–0.83 dL/g, and the weight-average molecular weights (Mw) and number-average molecular weights (Mn) values were recorded in the range of 34 000–67 000 and 18 000–35 000, respectively, relative to standard polystyrene (Table S2†).

The thermal properties of all the polyamides were investigated by TGA, DSC and TMA. The results are summarized in Table 1. All the polymers exhibited good thermal stability with insignificant weight loss up to 450 °C in nitrogen. The 10% weight-loss temperatures of the polyamides in nitrogen and air were recorded in the range of 490–530 and 510–540 °C, respectively. The amount of carbonized residue (char yield) of these polymers in nitrogen atmosphere was more than 66% at 800 °C. The high char yields of these polymers can be ascribed to their high aromatic content. All the polymers indicated no clear melting endotherms up to the decomposition temperatures on the DSC thermograms. This result also supports the amorphous nature of these TPA-containing polymers. The T_gs of all the polymers were measured to be in the range of 233–308 °C by DSC. The softening temperatures (T_s) of the polymer film samples were determined by the TMA method with a loaded penetration probe. They were obtained from the onset temperature of the probe displacement on the TMA trace. In all cases, the T_s values obtained by TMA are comparable to the T_g values measured by the DSC experiments. The typical TMA thermogram for polyamide **6a** and TGA curves for polyamide **6b** are shown in Fig. S9.†

Comparing the thermal properties data of polyamides **6** in Table 1, one will find that polyamide **6c** showed the highest T_g and T_s due to the attachment of bulky lateral fluorene groups thus restricting the segmental mobility. In addition, polyamide **6d** (without 4-methoxy substitution) revealed a slightly higher T_g and T_s than polyamide **6e** (with 4-methoxy substitution). It means that the bulky di(4-methoxyphenyl) substituent in polyamide **6e** increasing the steric hindrance for close chain packing, as well as an enhanced fractional free volume between polymer chains. Similar tendencies were observed with polyamides **6f** and **6g**; *i.e.*, polyamides **6f** showed the higher T_g and T_s than polyamide **6g**.

Optical and electrochemical properties

The optical and electrochemical properties of the polyamides were investigated by UV-vis and photoluminescence spectroscopy, and cyclic voltammetry. The results are summarized in Tables 2 and 3. The UV-vis absorption spectra of these polymers exhibited strong absorption bands at 351–363 nm in NMP solution, which are assignable to a π–π* transition resulting from the conjugation between the aromatic rings and nitrogen atoms. In the solution photoluminescence spectra, polyamides exhibited fluorescence emission at (450–504 nm). The polymer films were measured for optical transparency using UV-

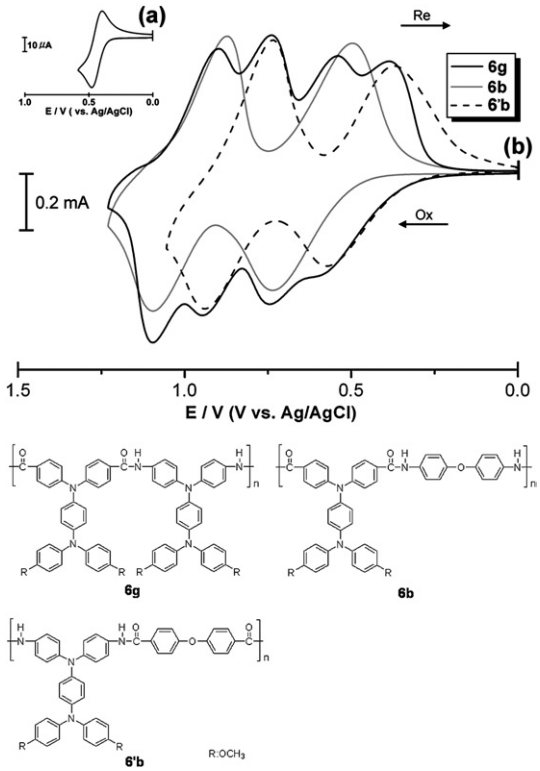

Fig. 1 Cyclic voltammograms of (a) ferrocene (b) polyamides **6g**, **6b** and **6′b** in CH_3CN containing 0.1 M TBAP at scan rate = 0.05 V/s.

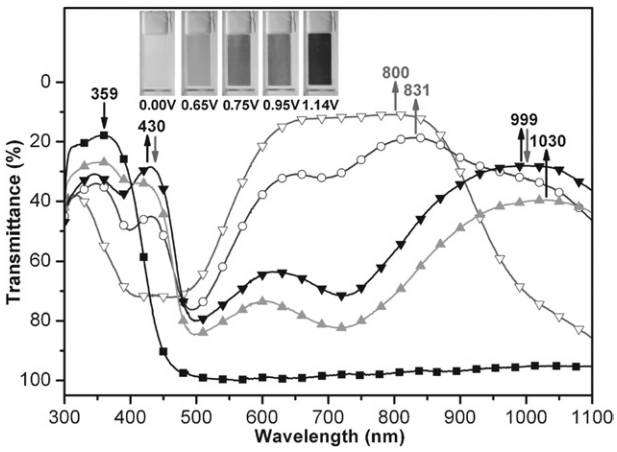

Fig. 2 Electrochromic behavior of polyamide **6g** thin film (in CH_3CN with 0.1 M TBAP as the supporting electrolyte) at 0.00 (■), 0.65 (●), 0.75 (▲), 0.95 (□), and 1.14 (○) (V vs. Ag/AgCl). $\mathbf{6g}^{+}$ and $\mathbf{6g}^{2+}$: (solid symbols with black arrows); $\mathbf{6g}^{3+}$ and $\mathbf{6g}^{4+}$: (hollow symbols with gray arrows).

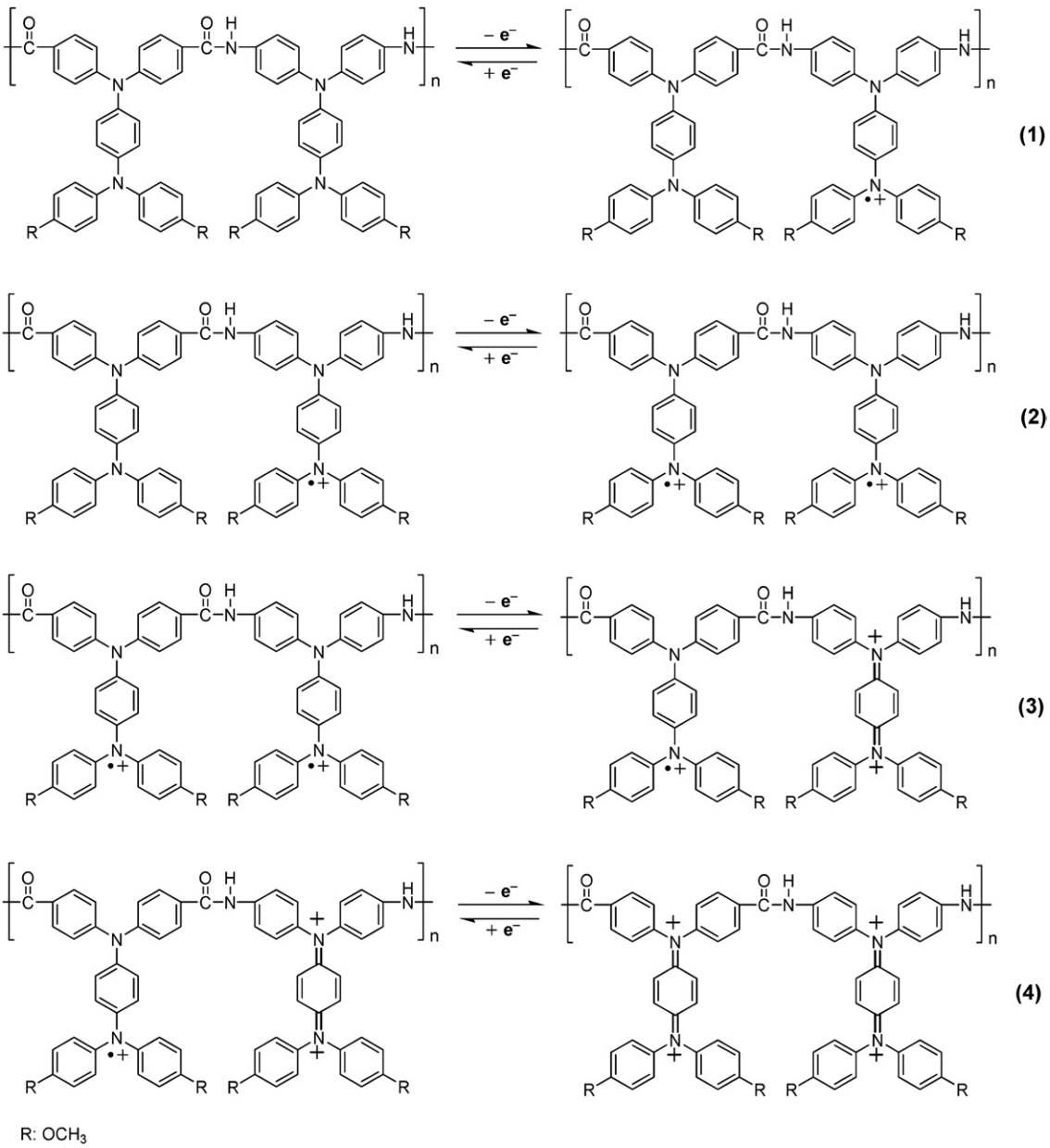

Scheme 3 The simplified redox process of polyamide **6g** from its neutral state, radical cation state to dication, trication and tetracation states.

vis spectroscopy, and the cutoff wavelengths (absorption edge; λ_0) were in the range of 405–419 nm (as shown in Fig. S10†).

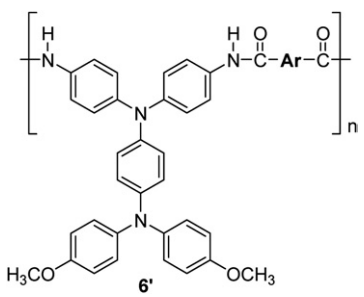

The electrochemical behavior of the polyamides **6** series was investigated by cyclic voltammetry conducted with film cast on an ITO-coated glass substrate as the working electrode in dry CH_3CN containing 0.1 M of TBAP as an electrolyte under nitrogen atmosphere. The typical cyclic voltammograms for polyamides **6g**, **6b** and **6′b** are shown in Fig. 1. There are four reversible oxidation redox couples for polyamide **6g** at E_{onset} = 0.35, $E_{1/2}$ = 0.64, 0.84, and 0.99 V corresponding to successive one electron removal from the nitrogen atoms at both *N*,*N*,*N*′,*N*′-tetraphenyl-1,4-phenylenediamine structures in each repeating unit to yield two stable delocalized radical cations, polyamide^{+} and polyamide^{3+}, from N atoms on the pendent and main chain TPA groups of the diamine, and two stable quinonoid-type dications, polyamide^{2+} and polyamide^{4+}, from N atoms on the pendent and main chain TPA groups of the diacid, respectively. Fig. S11† indicates electrochemical behavior for the model compounds and polyamides (**M1**, **M2**, **M3**, and **M4**), which have reversible oxidation redox couples at $E_{1/2}$ = 0.78

(E_{onset} = 0.70), 0.82 (E_{onset} = 0.73), 0.82 (E_{onset} = 0.68), 1.07 (E_{onset} = 0.90), respectively, to prove the oxidation order of nitrogen atoms for polyamide **6g**, and the results are summarized in Table 3. Comparing these electrochemical data, we found that polyamide **6g** (with 4-methoxy substitution) was much more easily oxidized than polyamide **6f** (without 4-methoxy substitution), and the first electron removal for polyamide **6g** could be assumed to occur at the pendent 4,4′-dimethoxytriphenylamine group, which is electron-richer than the N atom on the main chain TPA unit. Similar tendencies were observed with polyimides **6d** and **6e**; *i.e.*, polyamide **6e** was much more easily oxidized than polyamide **6d**. Because of the good stability of the films and excellent adhesion between the polymer and ITO substrate, these polyamides exhibited great reversibility of electrochromic characteristics by continuous cyclic scans between 0.0 and 1.20 V, changing color from the original pale yellowish to green, and then to blue. The energies of the highest occupied molecular orbital (HOMO) and lowest unoccupied molecular orbital (LUMO) levels of the investigated polyamides can be determined from the oxidation onset potentials and the onset absorption wavelength, and the results are listed in Tables 2 and 3. For example (Fig. 1), the oxidation onset potential for polyamide **6g** has been determined as 0.35 V vs. Ag/AgCl. The external ferrocene/ferrocenium (Fc/Fc^+) redox standard $E_{1/2}$ is 0.44 V vs. Ag/AgCl in CH_3CN. Assuming that the HOMO energy for the Fc/Fc^+ standard is 4.80 eV with respect to the zero vacuum level, the HOMO energy for polyamide **6g** has been evaluated to be 4.71 eV.

Electrochromic characterization

Electrochromism of the polyamide thin films was examined by an optically transparent thin-layer electrode (OTTLE) coupled with a UV-vis spectroscopy. The electrode preparations and solution conditions were identical to those used in cyclic voltammetry. The typical electrochromic absorption spectra of polyamide **6g** are shown as Fig. 2. When the applied potentials increased positively from 0 to 0.65, 0.75, 0.95, 1.14 V, respectively, corresponding to the first, second, third and fourth electron oxidation, the peak of characteristic absorbance at 359 nm for neutral form polyamide **6g** decreased gradually, while four new bands grew at 1030, 999, 831 and 800 nm, respectively. The new spectral patterns were assigned as those of the cationic radicals and quinonoid-type dications, the products obtained by electron removal from the lone pair of the nitrogen atom on two different *p*-phenylenediamine structures. According to the electron density of the four nitrogen atoms on two different *p*-phenylenediamine structures in each repeating unit, the anodic oxidation pathway of polyamide **6g** was postulated as in Scheme 3.

Meanwhile, the complementary color of the **6g** film changed from the original pale yellowish to green, and then to blue (as shown in Fig. 2) due to different oxidation states. After over 3000 cyclic switches to the green color, the films of polyamide **6g** showed excellent continuous cyclic stability of electrochromism (as shown in Fig. 3). The electrochromic characteristics of polyamide **6b** are also shown in Fig. 4. When the applied potentials increased positively from 0 to 0.85 V, the peak of transmittance at 357 nm, characteristic of neutral polyamide **6b**,

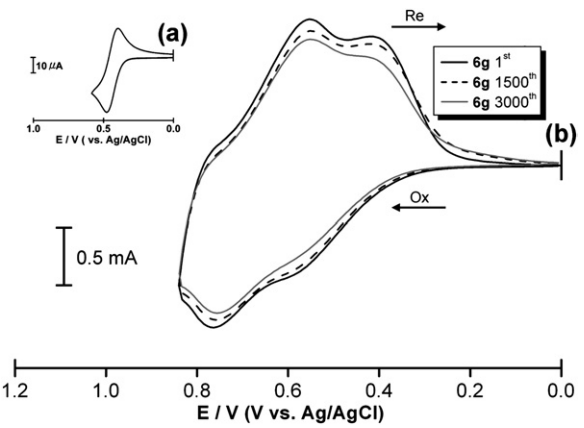

Fig. 3 Cyclic voltammograms of (a) ferrocene, (b) polyamide **6g** film on an indium-tin oxide (ITO)-coated glass substrate over 3000 cyclic scans in CH_3CN containing 0.1 M TBAP at scan rate = 0.08 V/s.

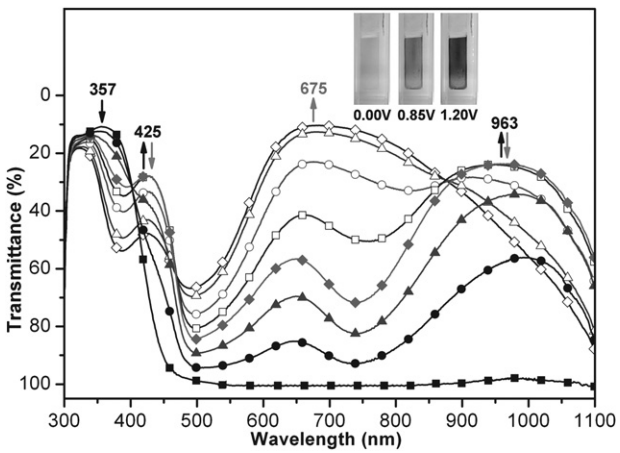

Fig. 4 Electrochromic behavior of polyamide **6b** thin film (in CH_3CN with 0.1 M TBAP as the supporting electrolyte) at 0.00 (■), 0.65 (●), 0.75 (▲), 0.85 (◆;), and 0.95 (□), 1.05 (○), 1.15 (△), 1.20 (◇) (V vs. Ag/AgCl). $\mathbf{6b}^+$: (solid symbols with black arrows) and $\mathbf{6b}^{2+}$: (hollow symbols with gray arrows).

decreased gradually. Two new bands grew at 425 and 963 nm due to the first stage oxidation. When the potential was adjusted to a more positive value of 1.20 V, corresponding to the second step oxidation, the peak of characteristic absorbance decreased gradually and a new band grew at 675 nm. Meanwhile, the film changed from colorless to green and then to a blue oxidized form. Polymer **6b** exhibited high contrast of optical transmittance change ($\Delta T\%$) to 74% at 963 nm for green and 89% at 675 nm for blue (as shown in Fig. 4). Thus, this will be a good approach for facile color tuning of the electrochromic behavior by attaching TPA units to the polymer main chain and/or as pendent groups.

The color switching times were estimated by applying a potential step, and the absorbance profiles were followed (Fig. 5 and 6). The switching time was defined as the time required to reach 90% of the full change in absorbance after the switching of the potential. Thin film from polyamide **6b** required 2.54 s at 0.88 V for switching absorbance at 425 and 963 nm and 1.37 s for bleaching. When the potential was set at 1.20 V, thin

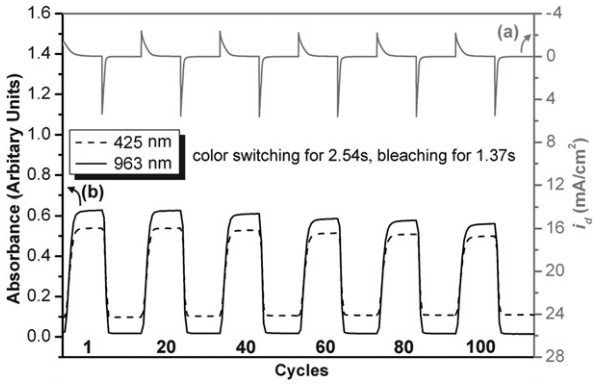

Fig. 5 (a) Current consumption and (b) potential step absorptometry of polyamide **6b** (in CH_3CN with 0.1 M TBAP as the supporting electrolyte) by applying a potential step (0.00 V ⇆ 0.88 V) (coated area: 1 cm^2) and cycle time 20s for coloration efficiency from 250 cm^2/C (1st cycle) to 239 cm^2/C (100th cycle).

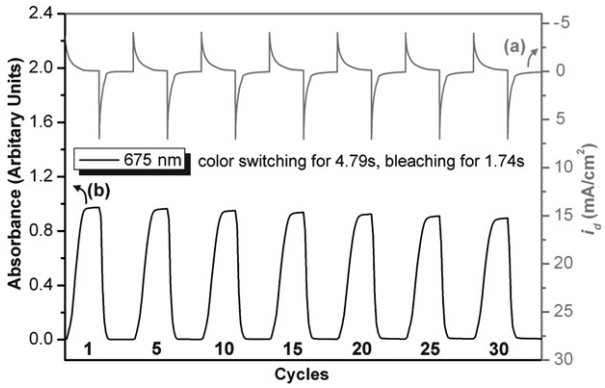

Fig. 6 (a) Current consumption and (b) potential step absorptometry of polyamide **6b** (in CH_3CN with 0.1 M TBAP as the supporting electrolyte) by applying a potential step (0.00 V ⇆ 1.20 V) (coated area: 1 cm^2) and cycle time 20s for coloration efficiency from 154 cm^2/C (1st cycle) to 141 cm^2/C (30th cycle).

film **6b** required 4.79 s for coloration at 675 nm and 1.74 s for bleaching. After over 500 cyclic switches for green color, the films of polyamide **6b** showed excellent continuous cyclic stability of electrochromism. The high electrochromic coloration efficiency of green ($\eta = \Delta OD_{963}/Q$) (250 cm^2/C for 1 cycle to 239 cm^2/C for 100 cycles) and blue ($\eta = \Delta OD_{675}/Q$) (154 cm^2/C for 1 cycle to 141 cm^2/C for 30 cycles) and decay of the polyamides **6b** were also calculated,[43] and the results are summarized in Table 4.

Table 4 Optical and electrochemical data collected for coloration efficiency measurements of polyamides **6b**

Cycles[a]	ΔOD_{963}[b]	Q[c]/mC cm^{-2}	η[d]/cm^2 C^{-1}	Decay (%)[e]
1	0.611	2.44	250	0
20	0.609	2.45	249	0
40	0.593	2.42	245	2
60	0.569	2.34	243	2.8
80	0.561	2.32	242	3.2
100	0.546	2.28	239	4.4

[a] Times of cyclic scan by applying potential steps: 0.00 ↔ 0.88 (V vs. Ag/AgCl) for **6b**. [b] Optical density change at 963 nm for **6b**. [c] Ejected charge, determined from the *in situ* experiments. [d] Coloration efficiency is derived from the equation: $\eta = \Delta OD/Q$. [e] Decay of coloration efficiency after cyclic scans.

Conclusion

A series of new polyamides **6a–6g** having TPA units both in the polymer main chain and as pendent groups have been readily prepared from the aromatic dicarboxylic acid, *N*,*N*-bis(4-carboxyphenyl)-*N*′,*N*′-di(4-methoxyphenyl)-1,4-phenylenediamine (**4**) and various aromatic diamines. Polymer **6b** exhibited high contrast of optical transmittance change (ΔT%) up to 74% at 963 nm for green and 89% at 675 nm for blue. After over 3000 cyclic switches for green color, the films of polyamide **6g** showed excellent continuous cyclic stability of electrochromism. By incorporating electron-donating methoxy substituents at the *para*-position of *N*,*N*,*N*′,*N*′-tetraphenyl-1,4-phenylenediamine, the oxidation potentials of the electroactive polyamides were lowered; this could be a good approach for facile color tuning of the electrochromic behavior due to the different multi-stage oxidation potentials. Attaching bulky electron-donating TPA units to the polymer main chain and/or as pendent groups can disrupt the coplanarity of aromatic units in chain packing, which increases the between-chains spaces or free volume, thus most of the polymers were amorphous with good solubility in many polar aprotic solvents. In addition to good thermal stability, all the obtained polyamides also revealed stability of electrochromic characteristics by electrochemical and spectroelectrochemical methods, changing color from the original pale yellowish to green, and then to blue. Thus, 4,4′-dimethoxy-substituted TPA-based polyamides could be good candidates as anodic electrochromic materials due to their useful oxidation potentials, excellent electrochemical stability, and thin film formability.

Acknowledgements

The authors are grateful to the National Science Council of the Republic of China for financial support of this work.

References

1 P. M. S. Monk, R. J. Mortimer and D. R. Rosseinsky, *Electrochromism: Fundamentals and Applications*, VCH, Weinheim, 1995.
2 C. G. Granqvist, A. Azens, J. Isidorsson, M. Kharrazi, L. Kullman, T. Lindstrom, G. A. Niklasson, C.-G. Ribbing, D. Roennow, M. Stromme Mattsson and M. Veszelei, *J. Non-Cryst. Solids*, 1997, **218**, 273.
3 P. M. S. Monk, *J. Electroanal. Chem.*, 1997, **432**, 175.
4 I. Schwendeman, R. Hickman, G. Sonmez, P. Schottland, K. Zong, D. M. Welsh and J. R. Reynolds, *Chem. Mater.*, 2002, **14**, 3118.
5 K. Bange, *Solar Energy Mater. Solar Cells*, 1999, **58**, 1.
6 C. G. Granqvist, A. Azens, A. Hjelm, L. Kullman, G. A. Niklasson, D. Ronnow, M. Stromme Mattsson, M. Veszelei and G. Vaivars, *Solar Energy*, 1998, **63**, 199.
7 S. A. Agnihotry, Pradeep and S. S. Sekhon, *Electrochim. Acta*, 1999, **44**, 3121.
8 R. D. Rauh, *Electrochim. Acta*, 1999, **44**, 3165.
9 C. E. Tracy, J. G. Zhang, D. K. Benson, A. W. Czanderna and S. K. Deb, *Electrochim. Acta*, 1999, **44**, 3195.
10 A. Pennisi, F. Simone, G. Barletta, G. Di Marco and M. Lanza, *Electrochim. Acta*, 1999, **44**, 3237.
11 D. L. Meeker, D. S. K. Mudigonda, J. M. Osborn, D. C. Loveday and J. P. Ferraris, *Macromolecules*, 1998, **31**, 2943.

12 D. S. K. Mudigonda, D. L. Meeker, D. C. Loveday, J. M. Osborn and J. P. Ferraris, *Polymer*, 1999, **40**, 3407.
13 I. D. Brotherson, D. S. K. Mudigonda, J. M. Ocborn, J. Belk, J. Chen, D. C. Loveday, J. L. Boehme, J. P. Ferraris and D. L. Meeker, *Electrochim. Acta*, 1999, **44**, 2993.
14 H. J. Byker, Gentex Corporation, *US Patent* No. 4902108.
15 R. J. Mortimer, *Chem. Soc. Rev.*, 1997, **26**, 147.
16 (*a*) K. Ogino, A. Kanagae, R. Yamaguchi, H. Sato and J. Kurtaja, *Macromol. Rapid. Commun*, 1999, **20**, 103; (*b*) W. L. Yu, J. Pei, W. Huang and A. Heeger, *J. Chem. Commun.*, 2000, **8**, 681; (*c*) M. Y. Chou, M. K. Leung, Y. O. Su, S. L. Chiang, C. C. Lin, J. H. Liu, C. K. Kuo and C. Y. Mou, *Chem. Mater.*, 2001, **16**, 654.
17 C. Creutz and H. Taube, *J. Am. Chem. Soc.*, 1973, **95**, 1086.
18 C. Lambert and G. Noll, *J. Am. Chem. Soc.*, 1999, **121**, 8434.
19 M. K. Leung, M. Y. Chou, Y. O. Su, C. L. Chiang, H. L. Chen, C. F. Yang, C. C. Yang, C. C. Lin and H. T. Chen, *Org. Lett.*, 2003, **5**, 839.
20 M. Robin and P. Day, *Adv. Inorg. Radiochem.*, 1967, **10**, 247.
21 A. V. Szeghalmi, M. Erdmann, V. Engel, M. Schmitt, S. Amthor, V. Kriegisch, G. Noll, R. Stahl, C. Lambert, D. Leusser, D. Stalke, M. Zabel and J. Popp, *J. Am. Chem. Soc.*, 2004, **126**, 7834.
22 F. Marken, C. M. Hayman and P. C. Bulman Page, *Electrochem. Commun.*, 2002, **4**, 462.
23 F. Marken, R. D. Webster, S. D. Bull and S. G. Davies, *J. Electroanal. Chem.*, 1997, **437**, 209.
24 J. D. Wadhawan, R. G. Evans, C. E. Banks, S. J. Wilkins, R. R. France, N. J. Oldham, A. J. Fairbanks, B. Wood, D. J. Walton, U. Schroder and R. G. Compton, *J. Phys. Chem. B*, 2002, **106**, 9619.
25 W. B. Davies, W. A. Svec, M. A. Ratner and M. R. Wasielewski, *Nature*, 1998, **396**, 60.
26 K. Y. Chiu, T. H. Su, C. W. Huang, G. S. Liou and S. H. Cheng, *J. Electroanal. Chem.*, 2005, **578**, 283.
27 (*a*) A. Kumar, D. M. Welsh, M. C. Morvant, F. Piroux, K. A. Abboud and J. R. Reynolds, *Chem. Mater.*, 1998, **10**, 896; (*b*) S. A. Sapp, G. A. Sotzing and J. R. Reynolds, *Chem. Mater.*, 1998, **10**, 2101; (*c*) D. M. Welsh, A. Kumar, E. W. Meijer and J. R. Reynolds, *Adv. Mater.*, 1999, **11**, 1379; (*d*) I. Schwendeman, R. Hickman, G. Sonmez, P. Schottland, K. Zong, D. M. Welsh and J. R. Reynolds, *Chem. Mater.*, 2002, **14**, 3118.
28 L. Hagopian, G. Kohler and R. I. Walter, *J. Phys. Chem.*, 1967, **71**, 2290.
29 A. Ito, H. Ino, K. Tanaka, K. Kanemoto and T. Kato, *J. Org. Chem.*, 2002, **67**, 491.
30 K. Y. Chiu, T. X. Su, J. H. Li, T. H. Lin, G. S. Liou and S. H. Cheng, *J. Electroanal. Chem.*, 2005, **575**, 95.
31 C. W. Chang, G. S. Liou and S. H. Hsiao, *J. Mater. Chem.*, 2007, **17**, 1007.
32 (*a*) G. S. Liou, S. H. Hsiao and T. H. Su, *J. Mater. Chem.*, 2005, **15**, 1812; (*b*) Y. Oishi, H. Takado, M. Yoneyama, M. Kakimoto and Y. Imai, *J. Polym. Sci., Part A: Polym. Chem*, 1990, **28**, 1763; (*c*) B. K. Spraul, S. Suresh, T. Sassa, M. Angeles Herranz, L. Echegoyen, T. Wada, D. Perahia and D. W. Smith Jr, *Tetrahedron Letters*, 2004, **45**, 3253.
33 R. Gujadhur, D. Venkataraman and J. T. Kintigh, *Tetrahedron Lett.*, 2001, **42**, 4791.
34 S. Urgaonkar, J. H. Xu and J. G. Verkade, *J. Org. Chem.*, 2003, **68**, 8416.
35 F. W. Bergstrom, I. M. Granara and V. Erickson, *J. Org. Chem.*, 1942, **7**, 98.
36 M. Yano, Y. Ishida, K. Aoyama, M. Tatsumi, K. Sato, D. Shiomi, A. Ichimura and T. Takui, *Synth. Met.*, 2003, **137**, 1275.
37 S. H. Cheng, S. H. Hsiao, T. H. Su and G. S. Liou, *Macromolecules*, 2005, **38**, 307.
38 G. S. Liou and C. W. Chang, *Macromolecules*, 2008, **41**, 1667.
39 (*a*) S. M. Pyo, S. I. Kim, T. J. Shin, H. K. Park, M. Ree, K. H. Park and J. S. Kang, *Macromolecules*, 1998, **31**, 4777; (*b*) J.-S. Kim, H. K. Ahn and M. Ree, *Tetrahedron Letters*, 2005, **46**, 277; (*c*) S. M. Pyo, S. I. Kim, T. J. Shin, M. Ree, K. H. Park and J. S. Kang, *Polymer*, 1998, **40**, 125; (*d*) T. J. Shin, H. K. Park, S. W. Lee, B. Lee, W. Oh, J.-S. Kim, S. Baek, Y.-T. Hwang, H.-C. Kim and M. Ree, *Polym. Eng. Sci.*, 2003, **46**, 1232; (*e*) S. M. Pyo, T. J. Shin, S. I. Kim and M. Ree, *Mol. Cryst. Liq. Cryst.*, 1998, **316**, 353.
40 J. N. Demas and G. A. Crosby, *J. Phys. Chem.*, 1971, **75**, 991.
41 N. Yamazaki, F. Higashi and J. Kawabata, *J. Polym. Sci. Polym. Chem. Ed.*, 1974, **12**, 2149.
42 N. Yamazaki, M. Matsumoto and F. Higashi, *J Polym. Sci. Polym. Chem. Ed.*, 1975, **13**, 1375.
43 R. J. Mortimer and J. R. Reynolds, *J. Mater. Chem.*, 2005, **15**, 2226.

